

Progressive Methods of Finishing the Dovetail Grooves of Aircraft Engine Compressor Disc

Natalia Honchar¹, Dmytro Pavlenko², Pavlo Tryshyn^{1*}, Olena Khavkina³

¹ Department of Mechanical Engineering Technology,
National University Zaporizhzhia Polytechnic, 64, Zhukovsky Str., Zaporizhzhia, 69063, UKRAINE

² Department of Aviation Engine Technology,
National University Zaporizhzhia Polytechnic, 64, Zhukovsky Str., Zaporizhzhia, 69063, UKRAINE

³ Department of Foreign Philology and Translation,
National University Zaporizhzhia Polytechnic, 64, Zhukovsky Str., Zaporizhzhia, 69063, UKRAINE

*Corresponding Author: trishin@zp.edu.ua

DOI: <https://doi.org/10.30880/ijie.2025.17.05.003>

Article Info

Received: 19 Jun 2024

Accepted: 14 February 2025

Available online: 30 August 2025

Keywords

Gas turbine engine, compressor disk, dovetail groove, fatigue, residual stress, nickel alloy, safety factor, finishing, hardening treatment

Abstract

The paper analyses the causes of compressor disc failures in aircraft engines. The high-pressure compressor discs were made of a nickel-based heat-resistant alloy, HN73MBTYu-VD. The complexity of the rim profile and the high level of loads create conditions for the development of fatigue cracks. Fractographic analysis of fractures has shown that the most dangerous cracks occur in the sharp corners at the base of the intergroove protrusions, which can lead to the tearing off of disc parts. The purpose of this study was to evaluate the effect of the optimal combination of finishing the groove forming surfaces on the safety factor of the rim elements of high-pressure compressor discs. Residual stresses were investigated by the layer-by-layer removal of thin metal layers using electrochemical polishing of the groove bottoms. To determine the stresses arising in the acute angle zone of the groove, the finite element method was used. The endurance limit of the specimens was determined after 2×10^7 loading cycles. It has been established that the optimal combination for the finishing stage of disc manufacturing includes sequential treatment with polymer-abrasive brushes, hardening with steel balls in an ultrasonic field, and pneumatic blasting with glass microbeads. Finish-hardening treatment improved resistance to fatigue crack nucleation by creating a certain depth of plastic deformation in the surface layer, inducing significant compressive residual stresses, improving surface roughness, and increasing microhardness. After this treatment, the safety factor of high-pressure compressor discs increases by 1.8 to 3 times. The paper presents a model for the safety factor of compressor discs with dovetail grooves, which takes into account technological residual stresses and operating conditions.

1. Introduction

One of the tasks of modern aircraft engine design is to ensure durability and reliability of highly loaded parts that limit the service life of gas turbine engines (GTE). The analysis of the literature devoted to the study of causes of failures of GTE critical parts has shown that 70-90% of all failures are of fatigue nature [1, 2, 3]. Despite the development of the metal fatigue science and structural and technological methods of increasing the endurance of GTE parts, the problem of fracture under the action of cyclic loads is still unsolved. It is particularly critical for

This is an open access article under the CC BY-NC-SA 4.0 license.



parts that have structural stress concentrators and are made of alloys that are highly sensitive to stress concentrations. The problem of fatigue failure is often exacerbated by difficult access to the stress concentration area, which complicates machining at the finishing stage of the manufacturing process.

One of the most characteristic GTE parts, for which these problems appear in sufficient degree, is compressor discs with dovetail grooves. The complexity of the rim profile of discs with angled grooves for the installation of working blades makes their mechanical and finishing machining much more difficult. In combination with a high level of static and cyclic loads under conditions of limited safety factor of discs, there are cases of their failure in operation. Complex cross-sectional transitions in the blade clamping grooves, being stress concentrators, create conditions for fatigue cracks.

The analysis of destroyed high-pressure compressor discs during operation has shown that the most common causes of their failure are fatigue failures [4, 5]. In this case, the fatigue crack nucleation centre can be located on the mating surfaces of both the groove and the intergroove protrusion (IGP). The structure of fractures also indicates the action of a high level of cyclic stresses in combination with a high level of constant stresses, contributing to the asymmetry of the loading cycle.

The results of fractographic analysis of crack fractures of the disc of the VI stage high-pressure compressor (Fig. 1, a) of the D-36 engine, taken out of service after 4925 hours of operation, and the disc after equivalent-cyclic tests, have shown that the greatest danger is cracking in the acute corner of the IGP base of dovetail grooves (Fig. 1, b). Under operating conditions, this leads to further crack development, mainly in the radial direction (Fig. 2), possible tearing off of several IGPs, and disc fracture. More rarely, the crack develops from an acute angle into the IGP body and leads to the separation of its part.

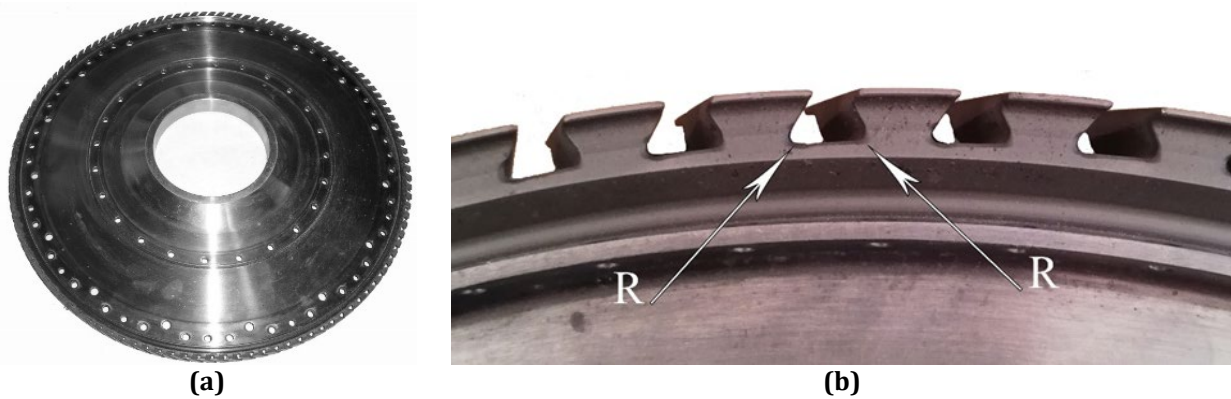


Fig. 1 General view of (a) High-pressure compressor disc; and (b) Of dovetail grooves

It has been found that the crack nucleation centre is located at the acute corner of the IGP base, on the surface of the radius R of the rounding between the bottom and the groove wall (Fig. 2, a). The crack developed transcrystallitically into the disc plate (Fig. 2, b). No structural defects have been identified. The failure was entirely of a fatigue nature.

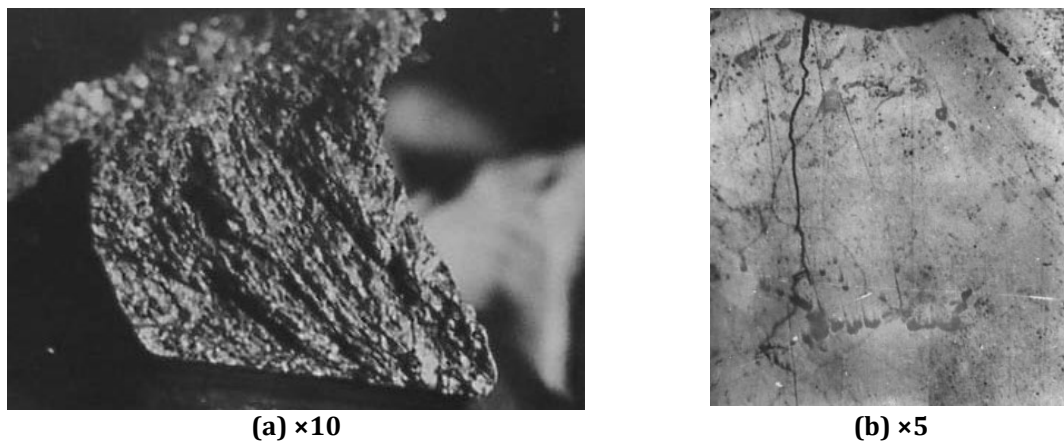


Fig. 2 IGP fracture: a general view of the fracture (a) and transcrystalline fracture development

Taking into account that the main operational parameter of compressor discs quality is the endurance limit, the increase of which increases the bearing capacity, and the stress concentrator is the dovetail grooves, the development of progressive finishing machining technology to increase the safety factor as the main characteristic of bearing capacity is an urgent task for aircraft engine building.

2. Literature Review

Currently, the main methods for investigating the endurance limit under the interaction of elevated temperature and combined tensile bending are experimental and numerical methods [6] and the finite element method [7, 8]. Applying the simulation modelling makes it possible to estimate the residual life of GTE parts, taking into account crack nucleation and development in critical areas [9]; the three-dimensional modelling [10, 11], neural network-based methods [12] and deep learning [13] are also used for this purpose.

The endurance limit of GTE parts largely depends on the condition of their surface layer, the characteristics of which differ significantly from the parameters of the core material, which many researchers point out [14, 15]. Surface atoms have one-sided bonds with the base material, so their state is unbalanced; they are more active and have excess energy, which creates conditions for interaction of the surface layer with the external environment (oxidation, adsorption, hydrogenation) [16].

The GTE parts fracture, in most cases, starts from the surface, where dislocations, vacancies, and slip bands are formed, leading eventually to fatigue cracking and fracture, usually on the side of the dovetail groove [17, 18]. Also, burrs in the dovetail grooves, which are a manufacturing defect of finishing, can be the cause of fatigue failure of high-pressure compressor discs [19]. The results of [20] showed that in turbine blades, most of the fatigue cracks were located along the near-surface carbides where they underwent grinding, burning, and then they propagated during service.

Investigating the influence of the stress state of the surface layer on endurance of GTE parts, the authors of [17] consider that the technological compressive residual stresses play the main role in its increase. Their influence is manifested in the inhibition of the process of nucleation and development of fatigue cracks in the surface, plastically deformed layer, by reducing the value of operational stresses and stress intensity factor at the tops of stress concentrators. The grinding analysis [21] has shown that the residual stresses in the crest areas were mainly tensile, whereas the residual stresses in the lower and bevelled areas were usually compressive.

One of the ways to increase the endurance limit of GTE parts may be the use of various methods of finishing and strengthening surface treatment. Basically, airblasting [18, 22], laser treatment [17, 23], and ultrasonic treatment [24, 25] are used as finishing processes for dovetail grooves. Finish-hardening treatment mainly improves resistance to fatigue crack nucleation by creating a certain depth of plastic deformation of the surface layer, significant compressive residual stresses, improving roughness and increasing microhardness [18, 19].

In [23] it was found that the fatigue life of Ti-6Al-4 V specimens after laser treatment increased by 14 %. In [24] it was shown that ultrasonic treatment of GH4169 superalloy increased the fatigue life by 3 times. And fatigue resistance was increased 4 times with pre-airblasting [26]. The microhardness and compressive residual stresses of the dovetail groove surface after airblasting are 16-27 % and 178-224 % higher, respectively, than in the initial state [18, 27, 28]. Treatment of complex surfaces of difficult-to-machine alloys with polymer-abrasive brushes (PABB) [29], which is able to create favourable compressive stresses in the surface layers and can also be used to automate the machining of hard-to-reach places of GTE parts, has proved itself to be effective.

However, despite the fact that existing studies of load-carrying capacity growth by means of finishing-hardening treatment have shown good results, practically all publications available to date are devoted to the treatment of laboratory specimens or simple-shaped parts. As for such studies of critical GTE parts, the overwhelming majority of them were performed for blades with specific features.

Of particular interest is the development of models of the strength reliability of such parts as high-pressure compressor discs with dovetail grooves, having a complex structural shape of the rim part and operating under cyclic loads, taking into account the action of residual stresses in the surface layer.

The purpose of this study was to evaluate the effect of the optimal combination of finishing the groove forming surfaces on the safety factor of the rim elements of high-pressure compressor discs.

3. A Model for Calculating the Safety Factor of High-Pressure Compressor Discs

Due to continuously increasing requirements to minimize GTE mass, their parts are becoming thin-walled, complex-profile, and their strength calculations are becoming more and more complicated. Sufficiently justified strength calculations of parts should take into account constructive, technological, and operational factors: operating modes, real properties of materials, loading conditions, presence of stress concentrators, etc. The complex stress state of the disc rim part is explained by a sharp change in the part configuration: the dovetail groove is a notch, which in turn has a transition radius R in its corners (Fig. 1, b). The grooves form intergroove protrusions (IGPs). It is also necessary to take into account the fact that the grooves are drawn at an angle of 40-

50° to the disc face. This results in the presence of a sharp angle at the base of the IGPs, where fatigue cracks mainly occur.

Various mathematical models related to the strength assessment of GTE parts have been proposed in the scientific literature. In [30, 31] various models for calculating the safety factor of GTE parts are proposed. Works [32, 33] present models for assessing the turbine disc residual life, taking into account the accumulated damage in the structure. The model [34] considers various combinations of rotation speed, temperature, shape, and size of surface defects, and titanium alloy properties. In [35], a model for fatigue life assessment of notched components under dimensional effects is proposed. The assessment of fatigue crack growth is fundamental to the development of advanced models, which are increasingly used as engineering tools for fatigue life prediction [36].

In the case of high-pressure compressor discs, various rim finishing methods can be used to modify the surface layer properties, which in turn affect the IGP fatigue resistance and finally the safety factor.

As initial data for building the model of influence of finishing and strengthening treatment technology on the safety factor, the following data were taken: endurance limits of full-scale specimens after different variants of finishing treatment technology, values of cyclic and constant stresses acting in the investigated zone of IGPs under normal and emergency modes of engine operation, and strength limit.

In the presence of stress concentration, taking into account the scale factor and surface condition, the model of endurance limit dependence in general is [37]:

$$\frac{k_{\sigma}}{\varepsilon\beta} \sigma'_a + \psi_{\sigma} \sigma'_m = \sigma_{-1} \quad (1)$$

One of the dependencies that determines the influence of a non-zero mean cycle stress is Smith's linear dependence [38]:

$$\sigma_a/\sigma_{-1} + \sigma_m/\sigma_B = 1 \quad (2)$$

Using the dependence elements (1) and (2), it was proposed that the value of the cyclic stresses should be calculated as:

$$\sigma'_a = \sigma_{-1} \cdot \frac{\varepsilon\beta}{K_{\sigma}} \cdot \left(1 - \frac{\sigma'_m}{\sigma_B}\right) \quad (3)$$

where σ'_a , σ'_m – are respectively the values of cyclic and constant stresses at the moment of fracture, MPa; σ_{-1} – is the endurance limit of full-scale specimens, MPa; σ_B – is the tensile strength of full-scale discs material, MPa; K_{σ} – is the effective stress concentration factor; ε – is the scale factor; β – is the complex coefficient that takes into account the influence of surface roughness and corrosion action.

The safety factor for a similar cycle (if the destructive and operating cycles are similar $\sigma'_a = n\sigma'_a$, $\sigma'_m = n\sigma'_m$) is calculated by the formula:

$$n_{sim} = \frac{\sigma_{-1}}{\frac{K_{\sigma}}{\varepsilon\beta} \cdot \sigma_a + \frac{\sigma_{-1}}{\sigma_B} \cdot \sigma_m} \quad (4)$$

where σ_a – is the value of cyclic stresses acting in the IGP base zone, at the place of the highest stress concentration; σ_m – is the constant stresses from centrifugal forces, gas flow pressure and temperature acting in the zone of IGP fracture at operating temperature, determining the loading cycle asymmetry, MPa.

The effective stress concentration factor K_{σ} characterises the difference between the stress concentration of the original part and the specimen. The coefficient ε takes into account the scale factor. In this case, $K_{\sigma}=1$ and $\varepsilon=1$, since the specimen is a full-scale one, cut from the compressor disc.

The coefficient β is taken as:

$$\beta = \beta_1 \cdot \beta_2 \quad (5)$$

where β_1 – is the coefficient, which considers the influence of corrosion. Taking into account that, according to the results of examination of the surface layer condition after a long-term operation, no traces of corrosion were detected, we take $\beta_1=1$; β_2 is the coefficient that takes into account the type of surface treatment and surface roughness. The studied surfaces of the specimens from different batches were of the same surface quality class, thus $\beta_2=1$.

Hence, the coefficient is $\beta = 1$.

Constant stresses on the surface σ_m , taking into account technological residual stresses, are proposed to be determined by the formula:

$$\sigma_m = \sigma_p + \sigma_{res} \quad (6)$$

where σ_p – is constant stresses in the stress concentrator zone at the groove base under operating conditions, MPa; σ_{res} – technological residual stresses on the groove surface that appeared during finishing operations, MPa.

In case if there are constant compressive stresses $\sigma_m < 0$ on the surface (taking into account technological residual stresses), the constant stresses were not taken into account when determining the safety factor, i.e. $\sigma_m = 0$.

If in the course of operation the IGP fracture occurs due to the increasing amplitude of only cyclic stresses ($\sigma_a' = n\sigma_a$, $\sigma_m' = \sigma_m$), then the safety factor is assessed by cyclic stresses:

$$n_a = \frac{\sigma_{-1} - \frac{\sigma_{-1}}{\sigma_b} \cdot \sigma_m}{\frac{K_\sigma}{\varepsilon\beta} \cdot \sigma_a} \quad (7)$$

Permissible safety factor values are accepted [39] for similar cycle [n_{sim}]=1.5-2 and for cyclic stresses [n_a]=2.5-4.

4. Materials and Methods

4.1 Object of Investigation

High-pressure compressor discs of the last stages operate under the most unfavourable conditions: maximum rotational speed is 14160 rpm; operating temperature reaches 550°C (data are given for the disc of the 6th stage of the high-pressure compressor for D-36 aircraft engine). Total stresses in grooves in the maximum stress concentration zone are 120 MPa. The dovetail grooves are located at an angle of 50°. In a normal cross-section, the width between the groove walls is 5.5 mm, the minimum width is 3.7 mm (Fig. 1, b). The working surfaces are located at an angle of 60°. The radius R is equal to 0.6-0.8 mm (Fig. 1, b). On the end of the disc and the bottoms of the groove a chamfer 0.5-0.3×45° mm or rounding radius r 0.5-0.6 mm is made to remove burrs and to round sharp edges left after broaching or re-broaching the grooves. The number of grooves along the disc rim is 117. The outer diameter of the high-pressure compressor disc is 462 mm.

The high-pressure compressor discs are made of nickel-based heat-resistant alloy HN73MBTYu-VD (62Ni-23Cr-11Co-5Mo-2Ti-1.5Al-2Fe), the physical and mechanical properties of which are given in Table 1. The closest analogues of the studied alloy by chemical composition and properties are nickel-based alloys Inconel 718, Waspaloy, Haynes 230, Rene 41, Udimet 720, and UNS07750.

Table 1 Physical and mechanical properties of HN73MBTYu-VD alloy [40]

Parameter	Meaning
Temperature t, °C	20
Elasticity modulus E, MPa	2×10 ⁵
Strength limit σ_b , MPa	1050
Yield strength $\sigma_{0.2}$, MPa	720
Relative elongation d, %	14
Relative contraction y, %	16
Impact strength KCU, κJ/m ²	4
Density r, kg/m ³	8320
Poisson's ratio m	0.3

The safety factor was estimated based on the loading of the disk IGPs by static forces from centrifugal forces, of blades inserted into the grooves, and of periodic forces arising from blade oscillation. The results of tensometric testing of the high-pressure compressor discs on the engine during its operation were used to calculate the stress state. Tensometers with 2 mm base were attached to the side surface A and the groove bottom B (Fig. 3). The stresses were determined at normal mode (at which the engine parameters change in time within the tolerances of technical specifications) and emergency mode (which is characterised by an increased value of engine power during 1-2 min without breakdown) of the discs in transient modes.

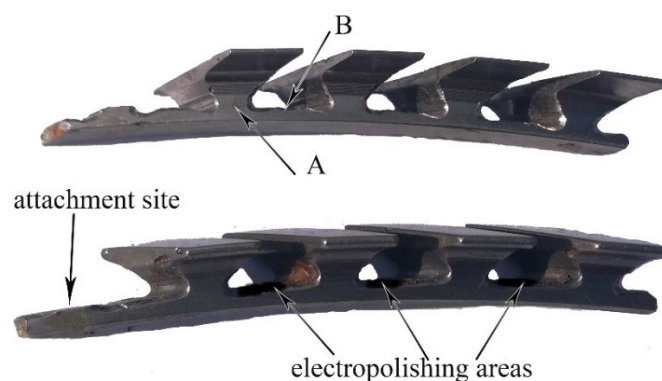


Fig. 3 Samples cut from the rim of a high-pressure compressor disc

Six batches of 10 full-scale specimens were used for the study (Fig. 3). They were cut from the rim part of newly manufactured high-pressure compressor discs after groove broaching, finishing and luminescent control and from end-of-life high-pressure compressor discs, which were restored using repair technology. The repair technology included groove re-broaching with increase of radius R (Fig. 1, b) up to 1-1.2 mm, finishing and luminescent control. At the same time, the efficiency of removing fatigue microcracks that appeared during operation of high-pressure compressor discs by re-broaching was investigated to prolong the discs service life.

4.2 Methods for Finishing Samples

Based on the analysis of existing research in the field of aircraft engine parts processing, main finishing methods suitable for processing dovetail grooves and adaptable to automation were selected. The high-pressure compressor discs were subjected to different combinations of these finishing treatments after broaching of grooves, which included:

1) Processing in a fluidised bed of abrasive (FBA) was carried out according to the batch technology for 8 min in a hermetically sealed chamber on a special installation at reversible rotation (90 sec in each direction) of the high-pressure compressor disc at a speed of 18-23 m/s; the depth of immersion in the fluidised bed was 0.25-0.5 diameter; the pressure in the chamber was 4-18 kPa. Working medium was grinding grain of electrocorundum with grain size 400-1000 microns.

2) Ultrasonic strengthening (USS). It was carried out with steel microballs of 0.68 mm diameter in a torus-type wave concentrator with reversible disc rotation at a peripheral velocity of 2.5 m/s for 16 min (8 min each way).

3) Processing with glass microballs on a pneumatic blast machine (PBM) was carried out sequentially, from both sides, with the following modes: pressure in front of the nozzle - 0.5 MPa; distance from the nozzle cut to the hardened surface - 15 mm. Glass microballs with a diameter of 40-70 microns were used. Processing time of high-pressure compressor discs was 15-80 s.

4) Processing with polymer-abrasive brush tools (PABT) of rotary action was carried out sequentially: firstly, burrs were removed using a disc PABT ($D=120$ mm, $B=10$ mm, fibre length of 12-20 mm, fibre diameter 1.0 mm, F80), then rounding of sharp edges between the disc face and the groove with radius of 0.5-0.6 mm was provided. Processing modes were as follows: cutting speed 17-20 m/s, feed $S = 1$ m/min, tension $i = 1-2$ mm, 5 passes with rotation reversal of the high-pressure compressor disc with each brush.

5) The groove re-broaching (RB) was carried out according to the repair technology, increasing the radius R from 0.6-0.8 mm to 1-1.2 mm, and removing the defective layer.

6) Metalworking (M) was used for deburring and blunting of sharp edges between the disc face and the groove bottom by chamfer $f=0.5-0.8$ mm with a tungsten carbide conical burr cutter with an angle at the apex of 90° manually using a pneumatic grinder.

4.3 Methodology for Studying the Distribution of Residual Stresses in the Bottom Part of the Disk Groove

Residual stresses were investigated by the method of layer-by-layer removal of thin metal layers [41, 30], by electrochemical polishing of the groove bottoms B (Fig. 3) on the specimens. For this purpose, on each specimen, the end intergroove protrusion at the very base was cut off by electro-erosion, providing an area for attachment. Residual stresses were investigated with the cantilever pattern of specimen fixation.

The value of residual stresses was calculated taking into account the stress components arising from the removal of the current layer and previous layers. The thickness of the removed layer was determined by weighing on analytical scales (before and after polishing). The total depth of polishing was up to 200-225 μm . In the process of successive removal of surface layers, the deflection of the specimen was continuously measured using a laser sensor.

4.4 Methodology for Testing Samples for Fatigue Strength under High-Cycle Loading

To determine the stresses arising in the acute angle zone of the groove, the finite element method was used with the help of the ANSYS program. For this purpose, the main volume of the 3D model was meshed with a free grid, while areas of stress concentration were meshed with a regular grid. The fastening and loading conditions corresponded to the operational ones.

The basing and fixing of the specimen for fatigue strength testing under multicycle loading was carried out on the IGP in a special device (Fig. 4).

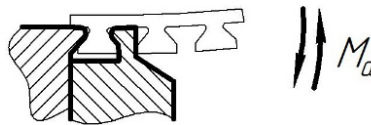


Fig. 4 Scheme of fixing and loading of the specimen on the vibration test bench

The specimen with the device attached in this way was mounted on the vibrator head of the electrodynamic vibration test bench. Thus, the fixing force did not create additional tension in the tested part of the specimen.

The specimens were dynamically set prior to testing.

During the tests, the vibration amplitude was maintained at the set level with an accuracy of ± 0.01 mm in automatic mode.

The endurance limit of the specimens was determined after of 2×10^7 loading cycles. Failure of the specimen was assessed by a 10% decrease in the frequency of natural vibrations at the appearance of a fatigue crack with a length of 0.2-0.4 mm.

5. Results and Discussion

During tensometric testing, the maximum values of constant (σ_r^*) and cyclic (σ_a^*) stresses were determined at A and B areas (Fig. 3) where the sensors were placed (Table 2).

Using the finite element method on the 3D model of the rim part of the high-pressure compressor disc (Fig. 5), the maximum values of stresses occurring in the zone of the groove acute angle for each finishing method were determined. Then, having the stress values of the two sections at tensometric testing during the operation of a real high-pressure compressor disc, the values of theoretical stress concentration coefficients in bending (α^*) and stretching (α^{**}) were determined. Based on the values of stress concentration coefficients, the values of constant (σ_r) and cyclic (σ_a) stresses obtained by computer calculation in the acute angle zone of the groove were specified (Table 2).

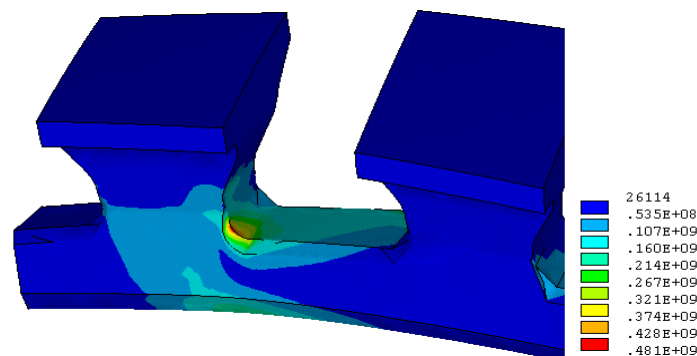


Fig. 5 Stress distribution (Pa) in the rim part of a high-pressure compressor disc under cantilever bending

Table 2 Calculation results

N ^o	Finishing variant	σ_a^* , MPa	α^*	σ_a , MPa	σ_m^* , MPa	α^{**}	σ_m , MPa
1	Broaching (without chamfer)	10.0	2.73	27.3	171.2	2.78	476.0
2	Broaching + M	10.0	1.38	13.8	171.2	1.51	258.5
3	Broaching + M + FBA	10.0	1.38	13.8	171.2	1.51	258.5
4	Broaching + M + USS	10.0	1.38	13.8	171.2	1.51	258.5
5	Broaching +PABT+ USS +PDM	10.0	1.29	12.9	171.2	1.39	237.9
6	Re-broaching + M + USS (for repair technology)	10.0	1.22	12.2	171.2	1.29	220.9

The results of examinations of endurance limit (σ_{-1}) and technological residual stresses (σ_{res}) of specimens after different finishing variants are given in Table 3.

Table 3 Test results

N ^o	Finishing variant	Normal mode		Emergency mode	
		σ_{res} , MPa	σ_{-1} , MPa	σ_{res} , MPa	σ_{-1} , MPa
1	Broaching (without chamfer)	300	100	300	100
2	Broaching + M	190	135	190	135
3	Broaching + M + FBA	-180	192	-180	192
4	Broaching + M + USS	-390	235	-390	235
5	Broaching +PABT+ USS +PDM	-460	244	-460	244
6	Re-broaching + M + USS (for repair technology)	-390	273	-390	273

Calculations using the proposed models (formula 6) show that high-pressure compressor discs with different combination of finishing treatments may have different safety factor, in some cases insufficient even for normal operation (Table 4).

Table 4 Result of calculating the safety factor of the high-pressure compressor disc

N ^o	Finishing variant	Normal mode				Emergency mode			
		σ_p , MPa	σ_m , MPa	n_{sim}	n_a	σ_p , MPa	σ_m , MPa	n_{sim}	n_a
1	Broaching (without chamfer)	476.0	776.0	1.06	1.19	476.0	776.0	0.67	0.40
2	Broaching + M	258.5	448.5	2.03	5.97	258.5	448.5	1.44	1.99
3	Broaching + M + FBA	258.5	78.5	6.03	10.81	258.5	78.5	2.98	3.60
4	Broaching + M + USS	258.5	0.0	13.48	13.48	258.5	0.0	4.49	4.49
5	Broaching +PABT+ USS +PBM	237.9	0.0	14.11	14.11	237.9	0.0	4.7	4.7
6	Re-broaching + M + USS (for repair technology)	220.9	0.0	17.72	17.72	220.9	0.0	5.91	5.91

The results of the research show that the specimens without chamfer have a safety factor insufficient for operation in any mode ($n_a=0.4$). At a sharp increase in temperature and load under conditions of emergency operation of a high-pressure compressor disc, the safety factor of specimens with a chamfer but without hardening decreases below the permissible ($[n_{sim}]=1.5-2$; $[n_a]=2.5-4$).

The FBA finishing treatment used to improve the surface layer quality of the disc rim increased the safety factor of the IGP's by 1.8 times over the initial ones, providing tolerance values.

USS due to induction of compressive residual stresses, absence of abrasive charging, and obtaining favourable microrelief provided a more significant increase in the safety factor under cyclic stresses and similar cycle by 2.25 times, which confirms the previously obtained results [24].

A slightly higher value of safety factors for both normal and emergency operation is provided by PABT treatment of the disc, followed by complex hardening.

Repeated broaching (re-broaching) with an increased radius R reduces the theoretical stress concentration factor at the base of the IGPs; the endurance limit increases by 10%, and the safety factor increases both for the similar cycle and for cyclic stresses. It should be noted that an excessive increase in radius R weakens the IGPs by reducing their base working cross-section.

Re-broaching using a repair technology that takes all of the above into account, followed by USS strengthening, by reducing the structural and process stress concentration in the danger zone, gives an additional increase in the safety factor of 3 times.

As a result, according to the investigated finishing and strengthening methods of processing high-pressure compressor discs, it can be said that the combination including sharp edge blunting using PABT [29], complex hardening (USS + PDM) provides the highest coefficient of safety factor under cyclic stresses and under similar cycle. As a result of the above, it can be stated that a qualitatively executed radius of rounding of the groove's sharp edge and an optimal radius R make it possible to significantly increase the safety factor of the IGPs under conditions of normal and emergency modes of engine operation.

6. Conclusion

The following conclusions can be made from this study:

1) The model of safety factor of high-pressure compressor discs with dovetail grooves, which takes into account technological residual stresses and operating mode, has been developed. This model is universal. Its work is shown on a specific example of a high-pressure compressor disc for the D-36 engine made of HN73MBTYu-VD alloy. However, it can be applied to other materials and designs of high-pressure compressor discs.

2) It has been established that the optimal combination of the finishing stage of disc manufacturing is the sequential treatment with polymer-abrasive brushes, hardening with steel balls in the ultrasonic field, and pneumoblast treatment with glass microballs. After this processing, the safety factor of high-pressure compressor discs increases by 1.8-3 times.

3) For the high-pressure compressor disc of the D-36 engine, a range of safety factor values (3.6-5.91) has been obtained depending on the applied finishing treatment. However, these values will be observed only at the initial moment of engine operation, and with the passage of time, they will decrease due to stress relaxation. This study has addressed the residual stress relaxation through a comprehensive approach that incorporates:

-Careful selection of variable and constant cycle stresses.

-Determination of the endurance limit using specimens subjected to extended thermal exposure (500 hours) at operating temperature (550°C).

This methodology allows for the natural progression of relaxation processes and their subsequent consideration in the overall assessment. The extended thermal exposure time and elevated temperature conditions were specifically chosen to ensure that the material reaches a quasi-stable state regarding residual stress relaxation, thus providing more reliable long-term predictions.

Acknowledgement

The work was supported by the National Research Foundation of Ukraine (project NO.2023.04/0098 "Development of practical recommendations for expanding the use of additive technologies for the production of parts and field repair of military equipment", 0124U003918).

Conflict of Interest

The authors declare that there is no conflict of interest regarding the publication of the paper.

Author Contribution

The authors are responsible for the study conception, research design, data collection, data analysis, result interpretation and manuscript drafting.

Reference

- [1] Raghavendra, K., et al. (2023). Metallurgical Investigation of a fractured low-pressure turbine rotor (LPTR) cover plate of an aeroengine. *Engineering Failure Analysis*, 154, 107637, <https://doi.org/10.1016/j.engfailanal.2023.107637>

- [2] Balli, O. (2021). Turbine wheel fracture analysis of Jet Fuel Starter (JFS) engine used on F16 military aircraft. *Engineering Failure Analysis*, 128, 105616, <https://doi.org/10.1016/j.engfailanal.2021.105616>
- [3] Radgolchin, M., Anbarsooz, M. (2023). Fatigue failure of centrifugal compressor impellers: a comprehensive review. *Engineering Failure Analysis*, 107592, <https://doi.org/10.1016/j.engfailanal.2023.107592>
- [4] Luo, S., Wu, S. (2016). Fatigue failure analysis of rotor compressor blades concerning the effect of rotating stall and surge. *Engineering Failure Analysis*, 68, 1–9. <https://doi.org/10.1016/j.engfailanal.2016.05.021>
- [5] Poursaeidi, E., Babaei, A., Behrouzshad, F., Arhani, M.M. (2013). Failure analysis of an axial compressor first row rotating blades. *Engineering Failure Analysis*, 28, 25-33, <https://doi.org/10.1016/j.engfailanal.2012.08.021>
- [6] Zhang, R., et al. (2022). An investigation of high and room temperature fretting fatigue of DD6-FGH96 dovetail joint in aero-engine: experimental and numerical analysis. *International Journal of Fatigue*, 154, 106537, <https://doi.org/10.1016/j.ijfatigue.2021.106537>
- [7] Zhao, J., et al. (2023). Elasto-plastic bending behavior of Ti-6Al-4V alloy under coupling conditions of elevated temperature and combined tension-bending. *Journal of Materials Research and Technology*, 26, 5360-5372, <https://doi.org/10.1016/j.jmrt.2023.08.200>
- [8] Wei, D. S., et al. (2019). Study of the variation of contact state near the contact boundary in a dovetail attachment under different loads. *Engineering Failure Analysis*, 105, 518-526, <https://doi.org/10.1016/j.engfailanal.2019.07.025>
- [9] Shlyannikov, V.N., Yarullin, R.R., Ishtyryakov, I.S. (2019). Failure analysis of an aircraft GTE compressor disk on the base of imitation modeling principles. *Procedia Structural Integrity*, 18, 322-329, <https://doi.org/10.1016/j.prostr.2019.08.172>
- [10] Mangardich, D., Abrari, F., Fawaz, Z. (2019). Modeling crack growth of an aircraft engine high pressure compressor blade under combined HCF and LCF loading. *Engineering Fracture Mechanics*, 214, 474-486, <https://doi.org/10.1016/j.engfracmech.2019.04.028>
- [11] Giannella, V., Citarella, R., Perrella, M., Shlyannikov, V. (2019). Surface crack modelling in an engine compressor disc. *Theoretical and Applied Fracture Mechanics*, 103, 102279, <https://doi.org/10.1016/j.tafmec.2019.102279>
- [12] Liu, Y., Yuan, H. (2023). A hierarchical mechanism-informed neural network approach for assessing fretting fatigue of dovetail joints. *International Journal of Fatigue*, 168, 107453, <https://doi.org/10.1016/j.ijfatigue.2022.107453>
- [13] Han, S., Khatir, S., Wahab, M. A. (2023). A deep learning approach to predict fretting fatigue crack initiation location. *Tribology International*, 185, 108528, <https://doi.org/10.1016/j.triboint.2023.108528>
- [14] Cesari, G., Panella, F. W., Pirinu, A. (2020). Stress/strain state for critical components of a jet engine aeronautical compressor. *Engineering Failure Analysis*, 116, 104745, <https://doi.org/10.1016/j.engfailanal.2020.104745>
- [15] Yarullin, R.R., Zakharov, A.P., Ishtyriakov, I.S. (2018). Nonlinear fracture resistance parameters for cracked aircraft GTE compressor disk. *Procedia Structural Integrity*, 13, 902-907, <https://doi.org/10.1016/j.prostr.2018.12.170>
- [16] Kang, H., et al. (2023). Connection stiffness modeling of rotating dovetailed blade with macro-micro interface topography. *European Journal of Mechanics-A/Solids*, 101, 105064, <https://doi.org/10.1016/j.euromechsol.2023.105064>
- [17] Xue, N.P., et al. (2023). Review on research progress and comparison of different residual stress strengthening methods for titanium alloys. *Engineering Failure Analysis*, 144, 106937, <https://doi.org/10.1016/j.engfailanal.2022.106937>
- [18] Yao, S. L., et al. (2023). Fretting fatigue life improvement of nickel-based superalloy GH4169 dovetail slots by deflecting abrasive waterjet peening process. *International Journal of Fatigue*, 175, 107832, <https://doi.org/10.1016/j.ijfatigue.2023.107832>
- [19] Saraçyakupoğlu, T. (2021). Failure analysis of J85-CAN-15 turbojet engine compressor disc. *Engineering Failure Analysis*, 119, 104975, <https://doi.org/10.1016/j.engfailanal.2020.104975>
- [20] Zhang, J., et al. (2022). Analysis on tenon tooth cracks of a second stage high-pressure turbine blade. *Engineering Failure Analysis*, 141, 106681, <https://doi.org/10.1016/j.engfailanal.2022.106681>

- [21] Chen, T., et al. (2022). On the residual stresses of turbine blade root of γ -TiAl intermetallic alloys induced by non-steady-state creep feed profile grinding. *Journal of Manufacturing Processes*, 82, 800-817, <https://doi.org/10.1016/j.jmapro.2022.08.051>
- [22] Yao, S. L., et al. (2023). Surface strengthening in confined spaces: a novel deflecting abrasive waterjet peening for improving the surface integrity of nickel-based superalloys GH4169. *Journal of Manufacturing Processes*, 85, 417-433, <https://doi.org/10.1016/j.jmapro.2022.11.050>
- [23] Gu, H., et al. (2023). Effect of laser shock peening on boring hole surface integrity and conformal contact fretting fatigue life of Ti-6Al-4 V alloy. *International Journal of Fatigue*, 166, 107241, <https://doi.org/10.1016/j.ijfatigue.2022.107241>
- [24] Yang, J., et al. (2020). The effect of ultrasonic surface rolling process on the fretting fatigue property of GH4169 superalloy. *International Journal of Fatigue*, 133, 105373, <https://doi.org/10.1016/j.ijfatigue.2019.105373>
- [25] Duan, Y., Qu, S., Jia, S., Li, X. (2021). Effects of ultrasonic surface rolling processing on microstructure and wear properties of high-carbon high-chromium steel. *Surface and Coatings Technology*, 422, 127531, <https://doi.org/10.1016/j.surfcoat.2021.127531>
- [26] Wang, J., Gao, Y., Wei, X. (2021). Investigations of the effects of combination treatments on the fretting fatigue resistance of GH4169 superalloy at an elevated temperature. *Surface and Coatings Technology*, 426, 127758, <https://doi.org/10.1016/j.surfcoat.2021.127758>
- [27] Yuan, T., et al. (2023). Improving high temperature fretting fatigue performance of nickel-based single crystal superalloy by shot peening. *International Journal of Fatigue*, 171, 107563, <https://doi.org/10.1016/j.ijfatigue.2023.107563>
- [28] Yang, Q., et al. (2018). Effect of shot-peening on the fretting wear and crack initiation behavior of Ti-6Al-4V dovetail joint specimens, *International Journal of Fatigue*, 107, 83-95, <https://doi.org/10.1016/j.ijfatigue.2017.10.020>
- [29] Honchar, N., Tryshyn, P., Stepanov, D., Khavkina, O. (2021). Effect of Abrasive Finishing on the Electrical Parameters of SB and Rectangular Waveguides. In: *Advances in design, simulation and manufacturing IV. DSMIE 2021. Lecture Notes in Mechanical Engineering*, 2, 395-404, http://dx.doi.org/10.1007/978-3-030-77719-7_39
- [30] Salehnasab, B., Poursaeidi, E. (2020). Mechanism and modeling of fatigue crack initiation and propagation in the directionally solidified CM186 LC blade of a gas turbine engine. *Engineering Fracture Mechanics*, 225, 106842, <https://doi.org/10.1016/j.engfracmech.2019.106842>
- [31] Ronchei, C., Vantadori, S. (2021). Notch fatigue life estimation of Ti-6Al-4V. *Engineering Failure Analysis*, 120, 105098, <https://doi.org/10.1016/j.engfailanal.2020.105098>
- [32] Shlyannikov, V., et al. (2021). Mixed-mode crack growth simulation in aviation engine compressor disk. *Engineering Fracture Mechanics*, 246, 107617, <https://doi.org/10.1016/j.engfracmech.2021.107617>
- [33] Zhenhua, Z. H. A. O., et al. (2021). Prediction of combined cycle fatigue life of TC11 alloy based on modified nonlinear cumulative damage model. *Chinese Journal of Aeronautics*, 34(7), 73-84, <https://doi.org/10.1016/j.cja.2020.10.021>
- [34] Shlyannikov, V.N., Ishtyryakov, I.S. (2019). Crack growth rate and lifetime prediction for aviation gas turbine engine compressor disk based on nonlinear fracture mechanics parameters. *Theoretical and Applied Fracture Mechanics*, 103, 102313, <https://doi.org/10.1016/j.tafmec.2019.102313>
- [35] Liao, D., et al. (2020). Probabilistic framework for fatigue life assessment of notched components under size effects. *International Journal of Mechanical Sciences*, 181, 105685, <https://doi.org/10.1016/j.ijmecsci.2020.105685>
- [36] Huang, X., Chen, C., Xuan, H. (2021). Experimental and analytical investigation for fatigue crack growth characteristics of an aero-engine fan disc. *International Journal of Fatigue*, 148, 106252, <https://doi.org/10.1016/j.ijfatigue.2021.106252>
- [37] Belyaev, M. S., Morozova, L. V., Markova, E. S., Yakusheva, N. A. (2017). Estimation of the high cycle fatigue behavior and type of fatigue failure of the VKS-180 high-resistance steel. *Inorganic Materials: Applied Research*, 8(4), 573-578. <https://doi.org/10.1134/S2075113317040037>
- [38] Ince, A., Glinka, G. (2011) A modification of Morrow and Smith-Watson-Topper mean stress correction models. *Fatigue & Fracture of Engineering Materials & Structures*, 34(11), 854-867, <https://doi.org/10.1111/j.1460-2695.2011.01577.x>

- [39] Wang, X., Shi, Q., Fan, W., Wang, R., Wang, L. (2019). Comparison of the reliability-based and safety factor methods for structural design. *Applied Mathematical Modelling*, 72, 68–84, <https://doi.org/10.1016/j.apm.2019.03.018>
- [40] Company “Auremo”. (2025, February 11). Alloy HN73MBTYu-VD (E1698) <https://auremo.biz/materials/splav-hn73mbtyu-ei698.html>
- [41] Surtee, I., Nobre, J.P. (2017). Residual Stress Redistribution due to Removal of Material Layers by Electrolytic Polishing. *Materials Research Proceedings*, 2, 593-598, <http://dx.doi.org/10.21741/9781945291173-10>